

Vibrational Contribution to the Thermodynamic Properties of Lithium Ion Batteries System: A First Principles Calculations

Xin Gong¹, Jinmei Huang¹, Yan Chen¹, Musheng Wu¹, Gang Liu¹, Xueling Lei¹, Jianxiong Liang², Hanbiao Cao², Fenjin Tang², Bo Xu^{1,3}, Chuying Ouyang^{1,3,*}

¹ Department of Physics, Jiangxi Normal University, Nanchang, 330022, P. R. China

² Jiangxi ZT New Energy Co. Ltd, Guangfeng, 334600, China

³ Key Laboratory for Advanced Functional Materials of Jiangxi Province, Nanchang, 330022, P. R. China

*E-mail: cyouyang@jxnu.edu.cn

Received: 11 June 2013 / Accepted: 3 July 2013 / Published: 1 August 2013

Although density functional theory has played important role in designing electrode materials for lithium ion batteries, it fails in correctly prediction of temperature dependant parameters of performance of the battery system that is more relevant in application. To simulate the temperature dependence of the thermodynamic parameters, the lattice vibrational energy should be included. In this paper, we calculated the lattice vibrational dynamic properties of the LiCoO₂/Li half battery system. We found that there is no imaginary frequency appeared when all Li atoms are removed, indicating that the bulk structure is stable upon Li removal. Furthermore, the vibration frequency of Co atom along the *ab*-plane is substantially increased after lithium is removed, due to the strengthened Co-O bonds. The vibrational entropy of the LiCoO₂ and its delithiated state Li_□CoO₂ is very close to each other. We show that the intercalation potential of the battery is altered noticeable when the lattice vibrational contribution is included.

Keywords: lithium ion batteries, average intercalation potential, phonon dispersion, temperature correction

1. INTRODUCTION

Pushed by the urgent need from the power supply of electric vehicles, the design and development of future advanced high energy density, high safety and low cost Li-ion batteries and its related materials become important to both the academic and industrial researchers. In the past decade, computational materials sciences have played important roles in accelerating the progress of designing of new electrode materials for Li-ion batteries [1-4]. Among various techniques used in computational

material sciences, first principles calculation is of most important because of its powerful functionalities in predicting materials structural [5-6], electronic [7, 8], magnetic [9, 10] and other properties [11]. Most of these first principles calculations are based on density functional theory, which calculates materials ground state properties. That is to say, all those properties predicted from first principles calculations are materials under 0 K [12, 13], and thus the thermodynamic aspect of materials can not be correctly predicted. However, lithium ion batteries normally work under environment temperature. Therefore, there exist certain errors between the first principles predictions and the batteries environment temperature performance. For example, LiMn_2O_4 cathode is cubic structure at room temperature, while first principles calculation can only reproduce its low temperature orthorhombic structure [14, 15].

In order to correctly predict the temperature dependant properties of materials, the lattice vibrational energy should be included [16, 17]. The lattice vibrational characteristics of materials for lithium ion batteries is less studied comparing to other extensively studied physical and electrochemical properties. In 1995, Frank et al [18] reported the calculation of phonon dispersion of alkali metals with *ab initio* force constant method and compared their theoretical predicted phonon data with experimental observations. In 2009, Shi et al. [19] studied the lattice dynamics of LiFePO_4 cathode and compared the vibrational frequencies with experimental optical data. Although there are some theoretical studies on the lattice vibration of materials for lithium ion batteries, further analysis of the phonon data or model of the temperature correction to thermodynamic parameters are not reported.

In this paper, we will consider the contribution of lattice vibrational energy to the thermodynamic parameters of LiCoO_2 material. After briefly introduction of the methodology we used for the computation and analysis of the phonon data, we present the entropy and vibrational contribution to the Helmholtz free energy of Li metal, LiCoO_2 and its delithiated state. Then, taking LiCoO_2/Li half battery as an example we show that the intercalation potential (operation voltage) of the battery can be changed noticeably when the operating temperature varies.

2. THEORY AND METHODOLOGY

In order to analysis the finite temperature thermodynamic properties of electrode materials of interest, we use the first-principles quasi-harmonic approach to describe the Helmholtz free energy $F(V, T)$ [20],

$$F(V, T) = E(V) + E_{ele}(V, T) + E_{vib}(V, T),$$

Where $E(V)$ is the static energy at 0 K without taking into account the zero-point energy, $E_{ele}(V, T)$ represents the thermal electronic contribution at V and T , and it contributes only in low temperature environment. $E_{vib}(V, T)$ is the lattice vibrational contribution, which can be calculated from the phonon free energy according to the Bose-Einstein's statistics:

$$F_{vib} = \frac{1}{2} \sum_i^{3N} \varepsilon_i + k_B T \sum_i^{3N} \ln(1 - e^{-\beta \varepsilon_i})$$

where $\varepsilon_i = h\nu_i$ is the phonon energy at different vibrational modes, ν_i is the vibrational frequency, and $\beta \equiv (k_B T)^{-1}$.

The ground state energy and forces in the present study is calculated by the Vienna *ab initio* simulation package (VASP) [21]. The ground state of the electronic structure is described with density functional theory (DFT) and the generalized gradient approximation [22] plus the Hubbard U (GGA+U). The U (the on-site coulomb term) value for the Co-3d state is selected to be 4.91 eV according to other reports [23], and it is showed that this value is suitable for the layered LiCoO₂ system from our past experiences [24, 25]. The phonon data are calculated through the force constant method, while the atomic Hellmann-Feynman forces are calculated with VASP.

The body centered cubic Li metal is modeled with the primitive cell and a 9×9×9 Monkhorst-Pack [26] scheme *k*-points mesh is used in our calculation. We also used primitive cells models for the LiCoO₂ and its delithated state denoted as Li_□CoO₂ together with 5×5×5 Monkhorst-Pack [26] scheme *k*-points meshes for the integration in the irreducible Brillouin zone. Energy cut-off for the plane waves is chosen to be 600 eV.

3. RESULTS AND DISCUSSION

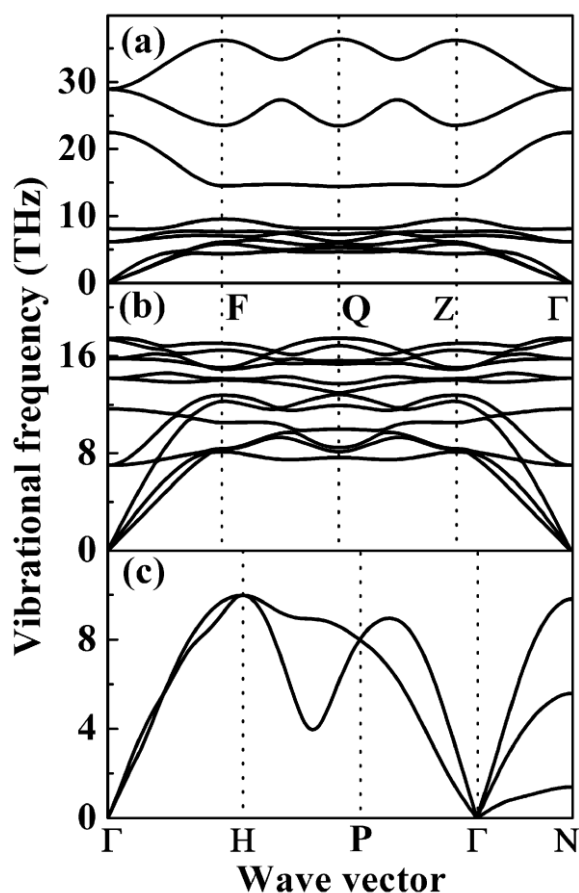


Figure 1. The phonon dispersion curves of (a) Li_□CoO₂, (b) LiCoO₂ and (c) metal Li in the first Brillouin Zone. High symmetry special *q*-points are marked with dotted lines.

The detailed information of lattice dynamics of solid materials can be obtained from the phonon dispersion curves. We calculated the phonon dispersion curves of LiCoO_2 (so as to its delithiated state $\text{Li}_\square\text{CoO}_2$) and metallic Li, as shown in Fig. 1. The crystalline Li metal has a body centered cubic lattice, and the primitive cell contains only one Li atom. Therefore, there are only three acoustic vibration modes, which are completely degenerate at the Γ , H, and P points in the Brillouin Zone. At the same time, the dispersion curves along lines between those high symmetry points are also degenerated and only two independent dispersion curves appeared. The highest vibrational frequency is about 9.98 THz, which is observed at the H-point. These results are in good agreements with reports in literature [18, 27].

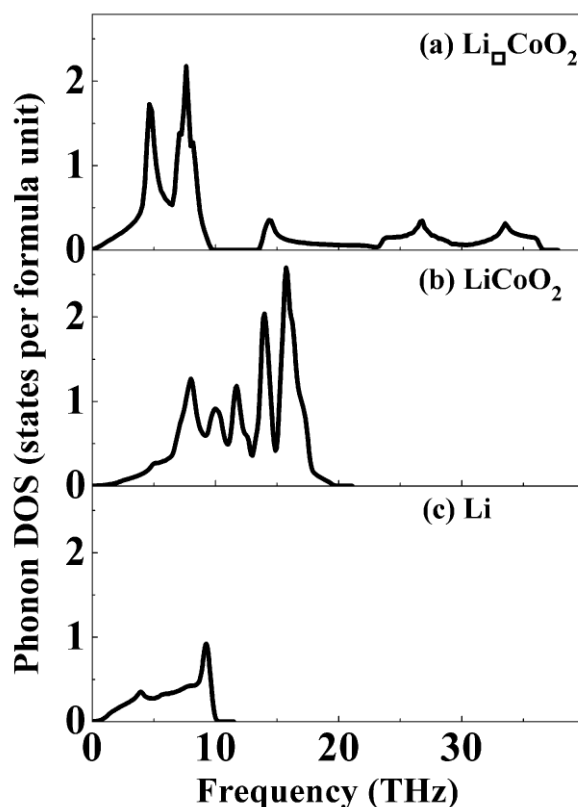


Figure 2. The phonon density of states of (a) $\text{Li}_\square\text{CoO}_2$, (b) LiCoO_2 , and (c) metal Li.

As the primitive cell of LiCoO_2 contains 4 atoms, there are nine optical branches and three acoustic branches in the phonon dispersion curves, as it is shown in Fig. 1b. The three acoustic vibration modes are complete degenerate at the Γ point ($q \rightarrow 0$, $\omega \rightarrow 0$), which represents the vibration of all atoms as a whole. The LiCoO_2 lattice has the point symmetry of D_{3d} . According to the symmetry, degenerate is also appear for the nine optical vibration modes and only five frequencies are shown at the Γ point. For the delithiated state $\text{Li}_\square\text{CoO}_2$, the point symmetry is retained and degeneration of the vibration modes is similar. Interestingly, we found that no imaginary frequency is appeared when all Li atoms are removed from the lattice, indicating that the bulk structure is stable upon lithium removal. Two vibration modes looks separated from the others, and its vibration frequency is close to 30 THz at

the Γ point. These two modes can be attributed to the vibration of Co atoms within the ab -plane (CoO_2 layer plane). After the lithium is extracted from the lattice, the oxidation state of Co changes from Co^{3+} to Co^{4+} and the Co-O bond lengths become shorter within the CoO_6 octahedral structure. The Co-O interaction becomes stronger, which enhances the vibration frequency substantially. On the other hand, the vibration frequency along the c -axis direction shifts to the low frequency region, because the lithium layer is completely removed from the lattice and the Coulomb interaction between the Li layer and the CoO_2 layer is disappeared.

To have a better comparison of the vibration frequency, the phonon density of states (DOS) is given in Fig. 2. Based on the phonon DOS data, we may calculate the vibrational contribution of the thermodynamic quantities, which directly associated with the intercalation potential of electrode materials for lithium ion batteries. The intercalation potential is originated from the Gibbs free energy changes of the battery system during the lithium intercalation process. Taking Li metal as anode and LiCoO_2 as cathode material, the intercalation potential can be calculated with [28, 29] $V_{ave} = \Delta G/nF$, where ΔG is the Gibbs free energy change of the intercalation reaction, F stands for the Faraday constant, and n represents the number of electrons (lithium ions) transferred in the intercalation process [30]. From thermodynamics we know that the Gibbs free energy includes the PV and the $-TS$ terms, in addition to the inner energy E . The Gibbs free energy is approximately chosen as equal to the inner energy when the intercalation voltage is calculated in the published literature [28, 29], because the $P\Delta V$ term is very small for solid state materials and the entropy contribution is zero when the temperature is 0 K. In the lithium ion battery system, it is reasonable to eliminate the contribution from the volume change because both the cathode and the anode materials are in solid state phase. Aydinol et al [29] estimated that the $P\Delta V$ term is of the order of 10^{-5} eV, which is negligible comparing the total Gibbs free energy change during the intercalation process (3 to 4 eV per formula lithium atom). However, the battery system generally operates under environmental temperature, from which the entropy contribution plays important role.

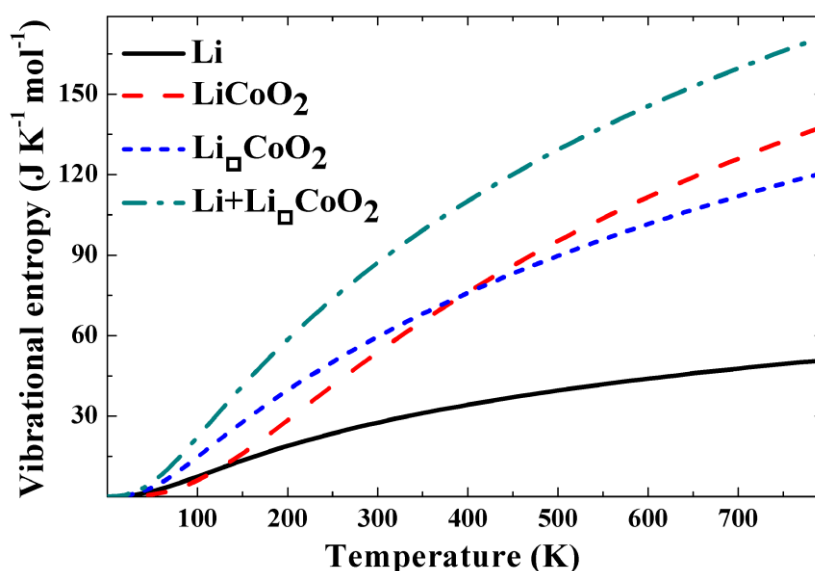


Figure 3. Vibrational entropies as a function of absolute temperature for Li metal, LiCoO_2 , $\text{Li}\square\text{CoO}_2$, and the delithiated system denoted as $\text{Li}+\text{Li}\square\text{CoO}_2$.

Taking the LiCoO_2/Li half battery as an example, Fig. 3 presents the vibrational entropies of different parts of the battery system. Interestingly, the vibrational entropy of the LiCoO_2 cathode is very close to that of its delithiated state $\text{Li}_\square\text{CoO}_2$, although LiCoO_2 has one more Li atom than $\text{Li}_\square\text{CoO}_2$ in one formula unit. The entropy of LiCoO_2 is even a little bit smaller than that of $\text{Li}_\square\text{CoO}_2$ when the temperature is below ~ 400 K. Therefore, we can see that lithium ion intercalated into the LiCoO_2 lattice does not increase the entropy of the compound. On the other hand, the entropy of lithium metal is quite large comparing to that of lithium ion in the LiCoO_2 lattice (note the different number of atoms in LiCoO_2 and Li formula units). As a result, the entropy increases upon charging (delithiation) of the LiCoO_2 cathode, namely, the entropy of the delithiated system, as denoted as $\text{Li}+\text{Li}_\square\text{CoO}_2$ in Fig. 3, is noticeably higher than that of the LiCoO_2 compound.

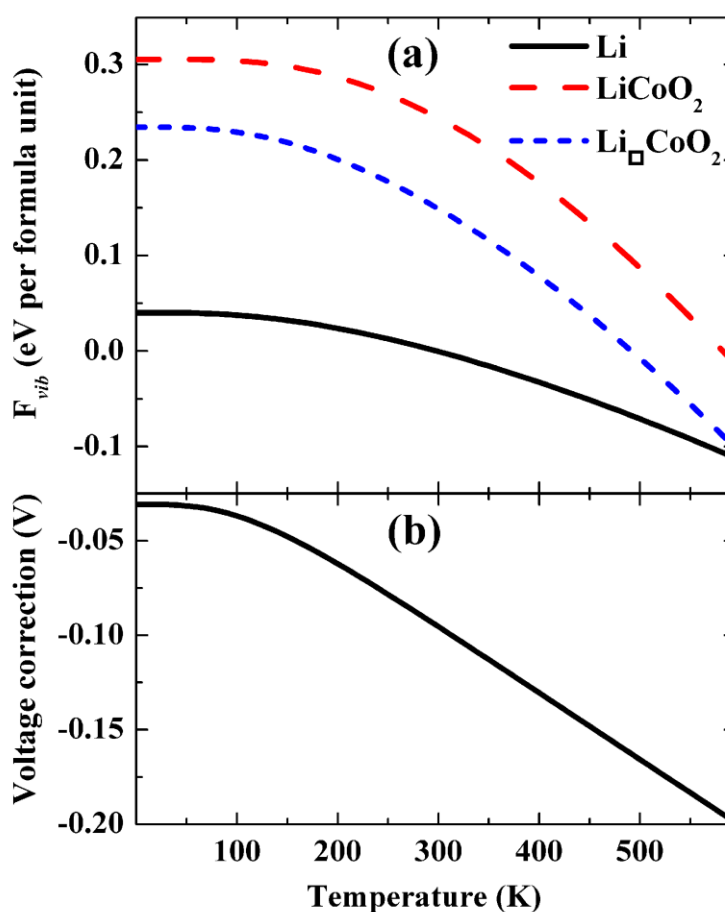


Figure 4. Vibrational free energies (a), and the intercalation voltage correction (b) as a function of the absolute temperature.

Figure 4a gives the vibrational free energies as a function of the temperature calculated from the phonon data. Taking into account the contribution of the zero point energies, we also calculated the intercalation potential correction of the LiCoO_2/Li half battery system operates at different temperature when the temperature effect is taking into account, as shown in Fig. 4b. Obviously, the intercalation potential decreases when the temperature increases. The correction is about 95 mV at 300 K. When the

temperature is increased to 350 K, the vibrational contribution to potential is about 113 mV. We mention here that although the potential correction due to the temperature effect is not large, it could be noticeable in terms of the performance change of the battery system. When the operation temperature increases from 300K to 350K, the voltage of the battery system will decrease 18 mV, which could result in a decrease of the discharge capacity by several percents.

4. SUMMARY AND CONCLUSION

In summary, we have shown that the lattice vibrational contribution can not be ignored when the temperature dependant performance of the battery system is evaluated. The phonon frequency difference between LiCoO_2 and its delithiated state $\text{Li}_\square\text{CoO}_2$ gives indirect evidence that the Co-O bonds are strengthened upon delithiation, which shows that the CoO_6 octahedral and thus the CoO_2 layers are quite stable even when the battery is deeply charged. After integration of the phonon DOSs data, we calculated the entropies and the vibrational Helmholtz free energies of Li metal, LiCoO_2 and $\text{Li}_\square\text{CoO}_2$, with which we evaluated the correction of the temperature effect to the intercalation potential of the battery system. Results show that the intercalation potential decreases noticeably when the temperature increases.

ACKNOWLEDGEMENT

Thanks to the support of NSFC under Grant Nos. 11064004, 11234013 and 11264014. C. Y. Ouyang is also supported by the "Gan-po talent 555" Project of Jiangxi Province and the oversea returned project from the Ministry of Education. Computations are partly performed at Tianjing High Performance Computer Center.

References

1. G. Ceder, Y. M. Chiang, D. R. Sadoway, M. K. Aydinol, Y. I. Jang, B. Huang, *Nature*, 392 (1998) 694.
2. C. Y. Ouyang, X. M. Zeng, Z. Sljivancanin, A. Baldereschi, *J. Phys. Chem. C*, 114 (2010) 4756.
3. G. Hautier, A. Jain, H. L. Chen, C. Moore, S. P. Ong, G. Ceder, *J. Mater. Chem.*, 21 (2011) 17147.
4. C. Y. Ouyang, D. Y. Wang, S. Q. Shi, Z. X. Wang, H. Li, X. J. Huang and L. Q. Chen, *Chin. phys. Lett.*, 23 (2006) 61.
5. S. Appalakondaiah, G. Vaitheeswaran, S. Lebegue, N. E. Christensen, A. Svane, *Phys. Rev. B*, 86 (2012) 035105.
6. Z. X. Nie, C. Y. Ouyang, J. Z. Chen, Z. Y. Zhong, Y. L. Du, D. S. Liu, S. Q. Shi, and M. S. Lei, *Solid State Commun.*, 150 (2010) 40.
7. D. A. Tompsett, D. S. Middlemiss, M. S. Islam, *Phys. Rev. B*, 86 (2012) 205126.
8. C. Y. Ouyang, Z. Y. Zhong, M. S. Lei, *Electrochem. Commun.*, 9 (2007) 1107.
9. D. N. Qian, Y. Hinuma, H. L. Chen, L. S. Du, K. J. Carroll, G. Ceder, C. P. Grey, Y. S. Meng, *J. Am. Chem. Soc.*, 134 (2012) 6096.
10. S. Q. Shi, C. Y. Ouyang, Z. H. Xiong, L. J. Liu, Z. X. Wang, H. Li, D. S. Wang, L. Q. Chen and X. J. Huang, *Phys. Rev. B* 71 (2005) 144404.
11. T. Maxisch, G. Ceder, *Phys. Rev. B*, 73 (2006) 174112.

12. Z. G. Mei, S. L. Shang, Y. Wang, Z. K. Liu, *Phys. Rev. B*, 79 (2009) 134102.
13. L. Wang, T. Maxisch, G. Ceder, *Chem. Mater.* 19 (2007) 543.
14. J. Rodriguez-Carvajal, G. Rousse, C. Masquelier, M. Hervieu, *Phys. Rev. Lett.*, 81 (1998) 4660.
15. C. Y. Ouyang, S. Q. Shi, and M. S. Lei, *J. Alloy Compound.*, 474 (2009) 370.
16. Z. G. Mei, S. L. Shang, Y. Wang, Z. K. Liu, *Phys. Rev. B*, 80 (2009) 104116.
17. P. P. Bose, M. K. Gupta, R. Mittal, S. Rols, S. N. Achary, A. K. Tyagi, S. L. Chaplot, *Phys. Rev. B*, 84 (2011) 094301.
18. W. Frank, C. Elsässer, and M. Fähnle, *Phys. Rev. Lett.*, 74 (1995) 1791.
19. S. Q. Shi, H. Zhang, X. Z. Ke, C. Y. Ouyang, M. S. Lei, and L. Q. Chen, *Phys. Lett. A*, 373 (2009) 4096.
20. S. L. Shang, Y. Wang, D. E. Kim, C. L. Zacherl, Y. Du, and Z. K. Liu, *Phys. Rev. B*, 83 (2011) 144204.
21. G. Kresse, J. Furthmüller, *Phys. Rev. B*, 54 (1996) 11169.
22. M.C. Payne, M.P. Teter, D.C. Allan, T.A. Arias, J.D. Joannopoulos, *Rev. Mod. Phys.*, 64 (1992) 1045.
23. I. V. Solovyev, P. H. Dederichs, V. I. Anisimov, *Phys. Rev. B*, 50 (1994) 16861.
24. F. Xiong, H. J. Yan, Y. Chen, B. Xu, J. X. Le, C. Y. Ouyang, *Int. J. Electrochem. Sci.*, 7 (2012) 9390.
25. J. M. Wang, J. P. Hu, C. Y. Ouyang, S. Q. Shi, M. S. Lei, *Solid State Commun.*, 151 (2011) 234.
26. H. J. Monkhorst, J. D. Pack, *Phys. Rev. B*, 13 (1976) 5188.
27. M. M. Beg, M. Nielsen, *Phys. Rev. B*, 14 (1976) 4266.
28. C. Wolverton, A. Zunger, *Phys. Rev. B*, 57 (1998) 2242.
29. M. K. Aydinol, A. F. Kohn, G. Ceder, K. Cho, J. Joannopoulos, *Phys. Rev. B*, 56 (1997) 1354.
30. Z. Y. Zhong, C. Y. Ouyang, S. Q. Shi, and M. S. Lei, *ChemPhysChem*, 9 (2008) 2104.